Nuclear Emissions During Acoustic Cavitation
(Supplement #2 for Science On-line)

R. P. Taleyarkhan,[1] C. D. West,[1,2] J. S. Cho,[3] R. T. Lahey, Jr.,[4] R. Nigmatulin[5],R. C. Block[4,2]

This supplement consists of a document entitled, "The Analysis of Bubble Implosion Dynamics", by R. I. Nigmatulin, R. I. Lahey*, Jr. and R. P. Taleyarkhan.

[1] Oak Ridge National Laboratory, Oak Ridge, TN 37831, USA. [2] Retired. [3] Oak Ridge Associated Universities, Oak Ridge, TN 37830, USA. [4] Rensselaer Polytechnic Institute, Troy, NY 12180, USA.   [5] Institute of Mechanics of Ufa—Bashkortostan Branch of Russian Academy of Sciences, 6, K. Marx St., Ufa, 450 000, Russia. * – corresponding author email: laheyr@rpi.edu.

SUPPLEMENT #2

THE ANALYSIS OF BUBBLE IMPLOSION DYNAMICS

Robert I. Nigmatulin
Russian Academy of Sciences
Ufa, Bashkortostan, Russia

Richard T. Lahey, Jr.
Rensselaer Polytechnic Institute,
Troy, NY, USA

Rusi P. Taleyarkhan
Oak Ridge National Laboratory,
Oak Ridge, TN, USA

The dynamics of a cavitation bubble was analyzed using a modified Rayleigh equation [Nigmatulin et al, 2000] for the slow (i.e., low Mach number) phase of the bubble growth and collapse transient, and a one-dimensional hydrodynamic shock (i.e., HYDRO) code was developed and used for the very rapid implosion phase (during which sonoluminescence and thermonuclear fusion may occur). The analytical model used in the HYDRO code was based on numerically evaluating the phasic conservation equations, and accounting for the interacting shock waves that may be formed within each phase.

For laser driven inertial confinement fusion, separate ion and electron temperatures are required to characterize the plasma during implosions. In contrast, in our case, the dissociation and ionization processes take place due to gas compression in the imploding bubble. During the ionization process the velocities of the ions and electrons are of the same order of magnitude, but the mass of the ions is much larger than that of the electrons. As a consequence, the main part of the thermal (i.e., internal) energy is associated with the ions. Moreover, bubble collapse lasts such a short time that the electrons are not able to absorb much thermal energy from the ions. Thus, the internal energy of the plasma in the bubble is almost equal the kinetic energy of ions, thus a single effective temperature should adequately characterizes the gas plasma. Clearly this is a simplification but it was deemed adequate to predict bubble implosion phenomena.

The one-dimensional phasic conservation equations in spherical coordinates are:

Gas Mass Conservation Equation

$$\frac{\partial \rho_g}{\partial t} + \frac{1}{r^2}\frac{\partial}{\partial r}\left(\rho_g u_g r^2\right) = 0. \tag{1}$$

Gas Momentum Conservation Equation

$$\frac{\partial \rho_g u_g}{\partial t} + \frac{1}{r^2}\frac{\partial}{\partial r}\left(\rho_g u_g^2 r^2\right) + \frac{\partial p_g}{\partial r} = 0. \tag{2}$$

Gas Energy Conservation Equation

$$\frac{\partial e_g}{\partial t} + \frac{1}{r^2}\frac{\partial}{\partial r}\left(u_g r^2\left(e_g + p_g\right)\right) = \frac{1}{r^2}\frac{\partial}{\partial r}\left(k_g r^2 \frac{\partial T_g}{\partial r}\right) \tag{3}$$

Liquid Mass Conservation Equation

$$\frac{\partial \rho_\ell}{\partial t} + \frac{1}{r^2}\frac{\partial}{\partial r}\left(\rho_\ell u_l r^2\right) = 0 \tag{4}$$

Liquid Momentum Conservation Equation

$$\frac{\partial \rho_\ell u_\ell}{\partial t} + \frac{1}{r^2}\frac{\partial}{\partial r}\left(\rho_\ell u_\ell^2 r^2\right) + \frac{\partial p_\ell}{\partial r} = 0. \tag{5}$$

Liquid Energy Conservation Equation

$$\frac{\partial e_\ell}{\partial t} + \frac{1}{r^2}\frac{\partial}{\partial r}\left(u_\ell r^2(e_\ell + p_\ell)\right) = \frac{1}{r^2}\frac{\partial}{\partial r}\left(k_\ell r^2 \frac{\partial T_\ell}{\partial r}\right) \tag{6}$$

In order to evaluate these conservation equations, we need equations of state, $p = p(\rho, T)$ and $\varepsilon = \varepsilon(\rho, T)$, which are valid over a wide range of pressures and temperatures.

EQUATIONS OF STATE

The Mie-Gruneisen equation of state for a highly compressed fluid is [Zeldovich & Raizer, 1966]:

$$\varepsilon = \left(e/\rho - u^2/2\right) = \varepsilon_p + \varepsilon_T, \quad p = p_p + p_T, \quad p_T = \rho\Gamma(\rho,T)\bar{c}_V T, \quad \varepsilon_T = \bar{c}_V(\rho,T)T \tag{7}$$

where ε_p and p_p are the potential, or "cold", components and ε_T and p_T are the thermal, or "hot" components of the internal energy and pressure, respectively, Γ is the Gruneisen coefficient, and $\bar{c}_V$ is an average heat capacity at constant volume.

The potential, or "cold", components characterize intermolecular force interactions, which depend on the average distances between the molecules that depend on the density, ρ. For rarefied gases, where these distances are very large (i.e., for small densities, ρ), the potential components are negligibly small. In contrast, the potential components (ε_p and p_p) are essential for dense gases (i.e., at high pressure) and for condensed (liquid and solid) states of matter. The thermal, or "hot", components (ε_T and p_T) characterize the internal energy and pressure due to thermal (chaotic) motion of the molecules. For many fluids, including acetone, the Gruneisen coefficient, Γ, depends only on density, ρ, i.e. $\Gamma = \Gamma(\rho)$.

The potential components can be represented by a Born-Mayer potential [Nigmatulin, 1991]:

$$p_p = A\left(\frac{\rho}{\rho_0}\right)^{2/3} \exp\left[b\left(1 - \left(\frac{\rho_0}{\rho}\right)^{1/3}\right)\right] - K\left(\frac{\rho}{\rho_0}\right)^{n+1} + \Delta p_p, \tag{8a}$$

3

$$\varepsilon_p = \frac{3A}{\rho_0 b} \exp\left[b\left(1 - \left(\frac{\rho_0}{\rho}\right)^{1/3}\right)\right] - \frac{3K}{\rho_0}\left(\frac{\rho}{\rho_0}\right)^n + \Delta\varepsilon_p .$$

(8b)

where, A, K, *b*, and *n* are constant coefficients, which completely specify the Born-Mayer potential, and $\Delta\varepsilon_p$ is the correction for potential energy.

To simulate thermal conductivity in an ionized gas, the thermal conductivity, k_g, was given by:

$$k_g = a_{1g}T^m + a_{2g}$$

(9)

where a_{1g}= 3.73 E-03, a_{2g}= -5.34 E-02, and *m*= 0.5. This model is expected to give a reasonable estimate of the molecular and electron conductivity of the gas and the associated heat loss.

We note that the different phases (e.g., liquid and vapor) can take place only for subcritical conditions. That is, for, $p < p_{cr}$, $T < T_{cr}$.

In our case (the supercompression of a vapor bubble in a liquid of the same substance), a difference between the liquid and vapor occurs when:

(1) The vapor density is smaller than the liquid density and pressures are low, in which case the potential corrections for the vapor state may not be important.

(2) The vapor in the bubble may have a much higher temperature than the liquid outside of the bubble. For instance, the maximum temperature of the liquid at the bubble interface may be of order of $10^3 - 10^4$ K, while at the same time, the maximum temperature of the vapor (i.e., the fluid which was a vapor when its pressure and its temperature were subcritical) near the center of the bubble may be predicted to the order of 10^6 K. That is why the analytical formulas for the thermal components of the same substance in the bubble ("vapor") and outside of the bubble ("liquid") can be different when the vapor is at a much higher temperature. For the above mentioned conditions we need to take into account the dissociation of the molecules and the ionization of the atoms in the vapor. This is done implicitly in the Equations of State.

For deuterated acetone (i.e., D-acetone: C_3D_6O) in the *nondissociated state*, the values of the parameters used in Eqs. (7) and (8) are:

$A = 0.111784 \times 10^9$ Pa, $K = 0.4935 \times 10^9$ Pa, $b = 16.541$, $\rho_0 = 858 \ kg/m^3$,
$\bar{M} = 0.064 \ kg/mol$, $\bar{c}_v = 2000 \ J/kg - K$.

$$n = 1, \quad \Delta p_p = 1.8195 \times 10^{15} \exp\left[-\left(\frac{\rho}{\rho_0}\right)^{-1}\bigg/0.035\right] Pa ,$$

$$\Delta\varepsilon_p = \int \frac{\Delta p_p(\rho)}{\rho^2} d\rho + 0.671815 \times 10^6 \ m^2/s^2$$

(10)

4

and the Gruneisen coefficient is given by:

$$\Gamma(\rho) = 0.66 - 0.053 \exp\left(-\frac{1}{0.287}\left(\frac{\rho}{\rho_0}\right)\right) - 0.15 \exp\left(-\frac{1}{0.14}\left(\frac{\rho}{\rho_0}\right)^2\right)$$

$$- 0.39 \exp\left(-\frac{1}{0.57}\left(\frac{\rho}{\rho_0}\right)^3\right) + 7.0 \exp\left(-\frac{1}{0.25}\left(\frac{\rho}{\rho_0}\right)^{-2}\right). \tag{11}$$

As can be seen in Figure-1, nondissociated deuterated acetone has a relatively steep shock adiabat, which is valid during rapid transients. That is, it was assumed that the process of dissociation for acetone does not occur during the very short collapse time associated with an implosion (i.e., the fluid molecules stay in their original nondissociated state).

A correction for the internal energy of *vapor* D-acetone must be used for $\rho < \rho_{crit}$ and $T < T_{crit}$:

$$\varepsilon_{T_{vap}} = \varepsilon_T + \Delta\varepsilon_T(T) \tag{12}$$

where,

$$\Delta\varepsilon_T(T) = \begin{cases} 5.0 \times 10^5 - 1000T \ m^2/s^2, \ for \ \rho < \rho_{crit}; T < T_{crit} \\ 0.0, otherwise \end{cases} \tag{13}$$

To model the fully *dissociated state* of D-acetone the parameters in the equations of state (i.e., Eqs. (7) and (8)) were again employed with the following parameters:

$A = 0.3666 \times 10^9$ Pa, $\quad K = 0.68 \times 10^9$ Pa, $b = 14.215$, $\quad \rho_0 = 858 \ kg/m^3$,

$n = 1/3$, $\bar{c}_v = 2000 \ J/kg - K$, $\quad \Gamma = 0.66$,

$$\Delta p_p = 0.6065 \times 10^{15} \exp\left[-\left(\frac{\rho}{\rho_0}\right)^{-1} \middle/ 0.035\right] \ Pa, \quad \Delta\varepsilon_p = \int\frac{\Delta p_p(\rho)}{\rho^2}d\rho + 0.74261 \times 10^6 \ m^2/s^2. \tag{14}$$

Figure-1 shows that the D-acetone equations of state agree with the available data [Trunin et al, 1992]. As noted before, due to the speed of the implosion process the frozen shock adiabat (i.e., the nondissociated EOS) for the liquid phase should be used.

It should also be noted that during the low Mach number stage of bubble dynamics the perfect gas law may be used for the vapor:

$$p_g = \rho_g R_g T_g, \quad \varepsilon_g = \bar{c}_V T_g, \quad and, \quad \gamma = \frac{(c_V + R_g)}{c_V} = 1.3 \tag{15}$$

At very high temperatures, where dissociation (D) and ionization (I) take place we used:

$$\varepsilon = (\varepsilon_p + \bar{c}_V T)(1 - \beta_D) + \beta_D\left[(1 - \beta_I)(\varepsilon_{pD} + c_{VD}T + \varepsilon_{D*}) + \beta_I(\varepsilon_I + \varepsilon_{I*})\right]$$
$$p = p(1 - \beta_D) + \beta_D\left[(1 - \beta_I)p_D + \beta_I p_I\right] \tag{16}$$

5

$$\varepsilon_I = c_{VI} T, \quad p_I = \rho \Gamma_I \varepsilon_I, \quad \Gamma_I = 0.66.$$

where the subscript "D" stands for dissociated fluid and "I" corresponds to ionized fluids, and for acetone:

$$T_D \approx 3{,}000 \text{ K} \qquad\qquad c_{VD} \approx 2{,}000 \text{ J/kg-K}$$
$$T_I \approx 120{,}000 \text{ K} \qquad\qquad c_{VI} \approx 8{,}000 \text{ J/kg-K}$$
$$\Gamma_D \approx 0.66$$

$$\beta_k = \exp\left(-\left(\frac{T_k}{2T}\right)^2\right), \quad (k = D, I),$$

and [Moss et al., 1994], $\varepsilon_{D*} = R\,T_D / \bar{M}$, $\varepsilon_{I*} = 2R\,T_I / \bar{M}$.

These equations were evaluated numerically using the following initial and boundary conditions for acoustically-driven bubble dynamics [Nigmatulin et al, 2000]:

Initial Conditions

$$u_g\big|_{t=0} = 0, \quad T_g\big|_{t=0} = T_{g0}, \quad p_g\big|_{t=0} = p_{gs}(T_{g0}), \quad \rho_g\big|_{t=0} = \rho_{g0},$$

$$u_\ell\big|_{t=0} = 0, \quad T_\ell\big|_{t=0} = T_{\ell 0}, \quad p_\ell\big|_{t=0} = p_{\ell 0}, \quad \rho_\ell\big|_{t=0} = \rho_{\ell 0} \tag{17}$$

Boundary Conditions

$$u_g\big|_{r=0} = 0, \quad \frac{\partial T_g}{\partial r}\Big|_{r=0} = 0, \quad \frac{\partial p_g}{\partial r}\Big|_{r=0} = 0 \tag{18}$$

$$u_g\big|_{r=a} = \dot{a} - \frac{m''}{\rho_g}, \quad u_\ell\big|_{r=a} = \dot{a} - \frac{m''}{\rho_\ell}, \quad p_g\big|_{r=a} = p_\ell\big|_{r=a} + \frac{2\sigma}{a} + \frac{4\mu_\ell u_\ell}{a}\Big|_{r=a} = p_\ell\Big|_{r=a} + \frac{2\sigma}{a} + \frac{4\mu_\ell}{a}\left(\dot{a} - \frac{m''}{\rho_\ell}\right),$$

$$k_\ell \frac{\partial T_1}{\partial r}\Big|_{r=a} - k_g \frac{\partial T_g}{\partial t}\Big|_{r=a} = m'' h_{fg}\left(p_g\big|_{r=a}\right) \tag{19}$$

$$T_\ell\big|_{r=a} - T_g\big|_{r=a} \equiv [T] = 0.45 \frac{m'' T_{sat}}{\sqrt{2R_g T_{sat} \rho_g\big|_{r=a}}} \tag{20}$$

where $r = a(t)$ is the location of the bubble interface.

The Hertz-Knudsen-Langmuir model for phase change [Schrage, 1953] is:

$$m'' = \frac{\alpha}{\sqrt{2\pi R_g}} \left(\frac{p_{sat}(T_\ell|_{r=a})}{\sqrt{T_\ell|_{r=a}}} - \frac{\chi p_g|_{r=a}}{\sqrt{T_g|_{r=a}}} \right) \tag{21}$$

where,

$$\chi = \exp(-\Omega^2) - \Omega\sqrt{\pi}\left(1 - \frac{2}{\sqrt{\pi}} \int_0^\Omega \exp(-x^2) dx \right) \tag{22}$$

$$\Omega = \frac{m''}{\sqrt{2} p_g|_{r=a}} \sqrt{R_g T_g|_{r=a}} = \frac{-\left(u_g|_{r=a} - \dot{a}\right)}{\sqrt{2 R_g T_g|_{r=a}}}; \tag{23}$$

The incident pressure in the far field, p_I, is given by [Nigmatulin et al, 2000]:

$$a\ddot{a} + \frac{3}{2}\dot{a}^2 = \frac{\left(p_\ell|_{r=a} - p_I\right)}{\rho_{\ell 0}} + \frac{a}{\rho_{10} C_\ell} \frac{d}{dt}\left(p_\ell|_{r=a} - p_I\right) \tag{24}$$

and the phase change coefficient, α, is related to the so-called accommodation coefficient [Kucherov et al., 1960], f, by:

$$\alpha = \frac{2f}{2-f} \tag{25}$$

NUMERICAL EVALUATIONS

The basic computation strategy was to use the modified Rayleigh equation given in Eq. (24) during that part of the bubble dynamics process in which the interfacial Mach number ($Ma_g \equiv |\dot{a}|/C_g$) is such that $Ma_g \leq 0.2$. At higher Mach numbers we switched over to the full HYDRO code simulation during the bubble implosion process. This approach was found to save a significant amount of computer time without sacrificing accuracy [Bae, 1999].

The slow (i.e., subsonic) portion of the bubble dynamics process was evaluated using a second order implicit scheme in time and space, the Dormann-Prince method [Hairer et al, 1987], which was applied to the model given in Eq. (24). Homobaric solutions of this type have been discussed at length by Nigmatulin et al [2000]. As noted previously, when the interfacial Mach number reached $Ma_g = 0.2$, the modified Rayleigh equation results were used to initialize the HYRDO code. The HYDRO code is comprised of the system of partial differential equations given in Eqs. (1) − (6), and, the equations of state and initial/boundary conditions given in Eqs. (7) − (23).

These partial differential equations were evaluated using a time splitting procedure and a first order Godunov scheme [Godunov et al, 1976] in mixed Eulerian-Langrangian coordinates. In addition, the set of equations was divided into two separate systems: the hydrodynamic system of equations (without considering heat transfer) was solved first, and then heat transfer was accounted for

during the second step. The solution of the hydrodynamic system of equations (i.e., the Euler equations), was based on a local Riemann problem for the coupled computational cells and the heat loss was implemented using a second order spatial approximation.

The ratio of the cell sizes in the gas and in the liquid at the bubble interface was chosen to satisfy: $\Delta r_\ell / \Delta r_v \approx \sqrt{\alpha_{T\ell}/\alpha_{Tv}}$, where $\alpha_T = k/c_p\rho$ for the liquid and vapor, respectively. The computational grid consisted of 500 equal sized cells inside the bubble and 1000 in the liquid zones, which were disposed geometrically according to the cell size ratio given above. To calculate the final stage of vapor bubble collapse more precisely, when the shock wave was focusing near the center of the bubble, we interpolated the results onto a 2000×2000 grid.

Figure-2 (the low Mach number stage) and Fig 3 (the high Mach number stage) show typical D-acetone results for two different forcing pressures. These incident pressures are composed of the acoustic forcing pressure the superimposed pressure due the shock waves caused by the bubbles in the cluster which collapse first [Tomita and Shima, 1990], the amplification of the compression waves due to the radial inertia induced by the oscillating bubbles [Nigmatulin, 1991], and/or the intensification of the shocks due to a nonuniform distribution of void fraction within the cluster [Akhatov et al, 1986]. As can be seen, increasing the magnitude of the net forcing pressure (i.e., from 100 bar to 200 bar) causes the peak gas/plasma temperature to increase about 21%. Due to the sensitivity of the weighted nuclear cross sections [Bosch and Hale, 1992] to temperature, this has a relatively strong effect on D-D neutron production [Nigmatulin et al , 2002].

Figure-4 shows typical predicted spatial distributions of pressure and temperature at several times (i.e., just before and after the shock wave reflects off itself at the center of the bubble). Interestingly, it was found that there is a rather small region near, but not at, the center of the imploding bubble where the potential for thermonuclear fusion neutron production is a maximum [Nigmatulin et al, 2002].

In accordance with the ORNL experimental results [Taleyarkhan et al, 2002], parametric runs showed peak gas temperatures that increased as the liquid pool temperature decreased and the phase change coefficient (α) increased. These observations indicate that a good fluid for bubble fusion is one that has a large value of α and can be run at high forcing pressures Δp (i.e., high liquid superheats) and at low liquid pool temperatures, T_0. D-acetone is such a fluid while heavy water (D_2O) is not. That is, acetone has a phase change coefficient (α) near unity [Paul, 1962], can be run at low liquid pool temperatures and experiments show that acetone can experience relatively large negative acoustic pressure amplitudes without giving rise to cavitation. In contrast, heavy water can not easily be put in tension without cavitation, will freeze as liquid pool temperature is reduced, and has a phase change coefficient, α, which is relatively low ($\alpha \cong 0.075$). Thus for heavy water a significant amount of vapor remains in the bubble during the implosion process, cushioning the collapse and mitigating the compression. Indeed, our HYDRO code computations show that for D_2O the peak gas temperatures are many times lower than for D-acetone.

Finally, to obtain an estimate of the D-D fusion neutron production rate, we may use the neutron kinetics equation of Gross [1984]:

$$\frac{dn_n'''}{dt} = \frac{1}{2}\left(n_D'''\right)^2 \left(\overline{\sigma v}\right) \tag{26}$$

where,

$$n_j''' = \quad \text{concentration of entity-j (i.e., j = D, ions/m}^3\text{; j = n, neutrons/m}^3\text{)}$$

$$\left(\overline{\sigma v}\right) = \text{weighted cross sections [Bosch and Hale, 1992]}$$

The neutron production per implosion may be determined from:

$$n_n = \int\limits_{t_{implosion}} dt \int\limits_{V_{bubble}} \frac{dn_n'''}{dt} dV \tag{27}$$

This integral may be estimated by using the Mean Value Theorem, yielding:

$$n_n \sim \left(n_{D_*}'''\right)^2 \left(\overline{\sigma v}\right)_* R_*^3 \Delta t_* \tag{28}$$

where R_* is the radius of the supercompressed/superheated central core region of the bubble, Δt_* is the reaction, time, and, depending on the modeling assumptions made, the range of the characteristic values are [Nigmatulin et. al, 2002], [Lahey et. al, 2002]:

$$n_{D_*}''' \approx 10^{29} \, \text{D/m}^3 \text{ (i.e., } \rho_* \approx 2.0 \times 10^3 \, \text{kg/m}^3 \text{)}, \quad \left(\overline{\sigma v}\right) \approx \left(10^{-32} \text{ to } 10^{-30}\right) \, \text{m}^3\text{/s (i.e.,}$$

$$T_* \approx \left(4 \text{ to } 7\right) \times 10^6 \, \text{K)}, \quad R_* \approx 1 \text{ to } 2\mu\text{m, and, } \Delta t_* \approx 10 \text{ to } 50 \text{ ps.} \tag{29}$$

Thus a reasonable estimate for the neutron production rate is:

$$n_n \approx 10^{-2} \text{ to } 10^1 \text{ neutrons/implosion.}$$

Since we expect about 1000 bubbles in the bubble clusters formed in the ORNL experiments, and each bubble cluster experienced up to 50 implosions/sec, having $n_n = 10^{-2}$ to 10 neutrons/implosion, implies:

$$\dot{n}_n = (1{,}000)(10^{-2} \text{ to } 10) \, (50) = 10^3 \text{ to } 10^6 \text{ neutrons/sec,}$$

which is in good agreement with what was measured in the ORNL experiments, [Taleyarkhan et. al, 2002].

It should be stressed that many modeling assumptions were necessarily made in the HYDRO code, such as: the equations of state, the use of an effective temperature to approximate the behavior of the electrons and ions in the plasma, the relevant energy losses, and the various mechanisms for shock wave intensification. There is no doubt that more realistic plasma physics, nuclear physics and thermal-hydraulic models can, and should, be developed for future applications (e.g., sonochemistry or

bubble fusion reactor design studies). Nevertheless, the predicted trends, and basic physical phenomena that have been modeled, agree with our experimental observations and are expected to be remain valid.

<u>REFERENCES</u>

Akhatov, I.S., Baikov, V.A., Baikov, R.A., "Propagation of nonlinear waves in gas-liquid media with a gas content variable in space", *Fluid Dynamics*, Vol. 21, No. 1, 1986.

Bae, S-H, "A Theoretical Investigation of the Dynamics of Single Bubble Sonoluminescence", PhD Thesis (Engineering Physics), Rensselaer Polytechnic Institute, 1999.

Bosch, H. S. and Hale, G. M., *Nuclear Fusion*, Vol. 32, p. 611, 1992.

Godunov, S.K., Zabrodin, A.V., Ivanov, M.Ya., Kraiko, A.N., Prokopov, G.P., "Numerical Solution of Gas Dynamics Multidimensional Problems," [in Russian]. Moscow, *Nauka*, 1976.

Gross, R.A., *Fusion Energy*, John Wiley & Sons, 1984.

Hairer, E., Norsett, S., Wanner, G. "Solving Ordinary Differential Equations. I. Nonstiff Problems," New York, 1987.

Kucherov, R. Ya. And Rikenglaz, L.E., "The Problem of Measuring the Condensation Coefficient," *Doklady Akad. Nauk.,* SSSR, Vol. 153, No. 5, pp. 1130-1131, 1960.

Lahey, R.T., Jr., Nigmatulin, R.I., and Taleyarkhan, R. P., "Sonoluminescence and the Search for Bubble Fusion" Proceedings of Heat-2002, 3rd Int. Conf. On Transport Phenomena in Mulitphase Systems, Kielce, Poland, 2002.

Moss, W. C., Clarke, D. B., White, J. W. and Young, D. A., "Hydrodynamic Simulations of Bubble Collapse and Picosecond Sonoluminescence", *Phys. of Fluids*, Vol. 6, 2979, 1994.

Nigmatulin, R.I., "Dynamics of Multiphase Media", Hemisphere, New York, 1991.

Nigmatulin, R.I., Akhatov, I.Sh., Vakhitova, N.K., and Lahey, R.T., Jr., "On the Forced Oscillations of a Small Gas Bubble in a Spherical Liquid-Filled Flask", *J. Fluid Mech.*, Vol. 414, pp. 47-73, 2000.

Nigmatulin, R. I., Akhatov, I., Lahey, R. T., Jr. and Taleyarkhan, R. P., "The Analysis of Bubble Fusion", to be published, *Physics of Fluids*, 2002.

Paul, B., "Evaporation coefficients", *Raketnaya Tekhnika*, No. 9, pp. 3-12, 1962.

Schrage, R. W., "A Theoretical Study of Interphase Mass Transfer", Columbia Univ. Press, N.Y., 1953.

Taleyarkhan, R. P., West, C. D., Cho, J. S., Lahey, R. T., Jr., Nigmatulin, R. I. and Block, R. C., "Evidence for Nuclear Emissions During Cavitation", In press, *Science*, 2002.

Tomita, Y. and Shima, A, "High-speed photography observations of laser-induced cavitation bubbles in water", *Acustica*, Vol. 71, 1990.

Trunin, R.F., Zhernokletov, M.V., Kuznetsov, N.F., Radchenko, O.A., Sichevskaya, N.V., and Shutov, V.V., "Compression of liquid organic substances in shock waves", [in Russian] *Khimicheskaya Fizika*, Vol. 11, No. 4, pp. 424-432, 1992.
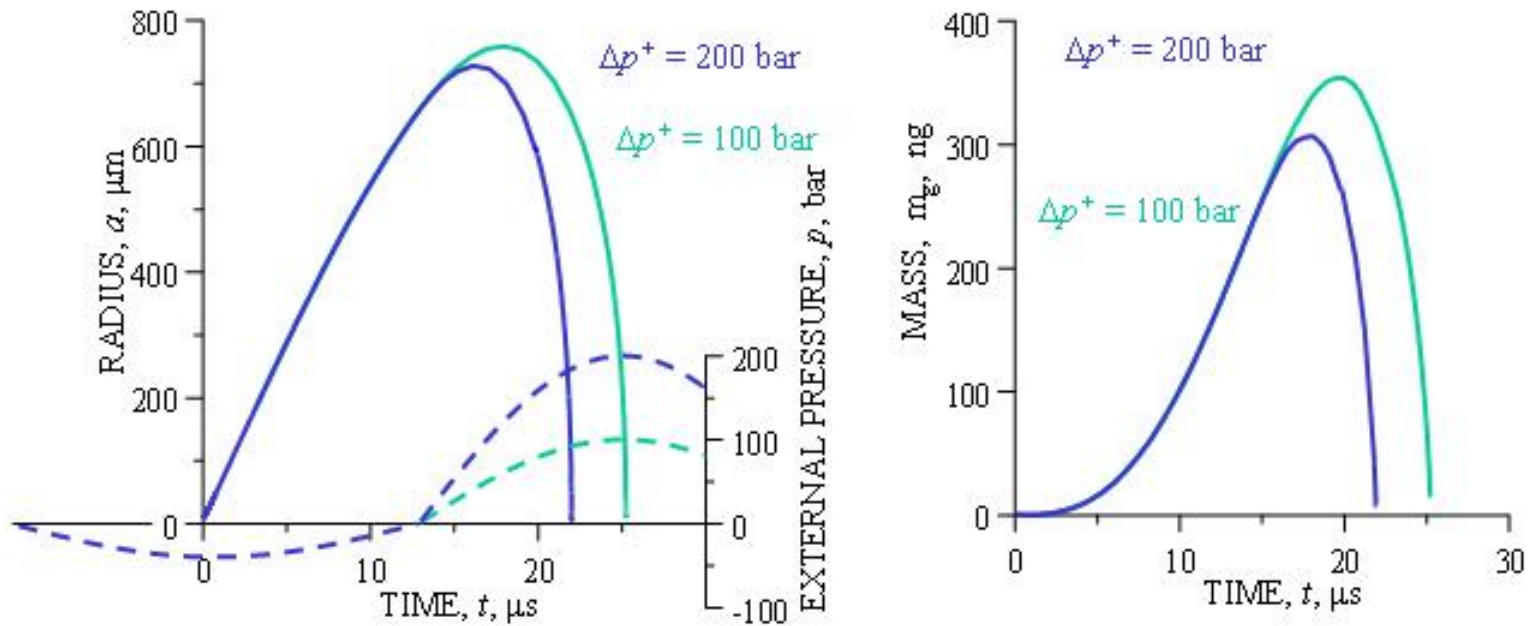
Zeldovich, Y.B., Raizer Y.P. "Physics of Shock Waves and High-Temperature Hydrodynamic Phenomena", Academic Press, New York, 1966.

Equation of state for Deuterated Acetone C_3D_6O
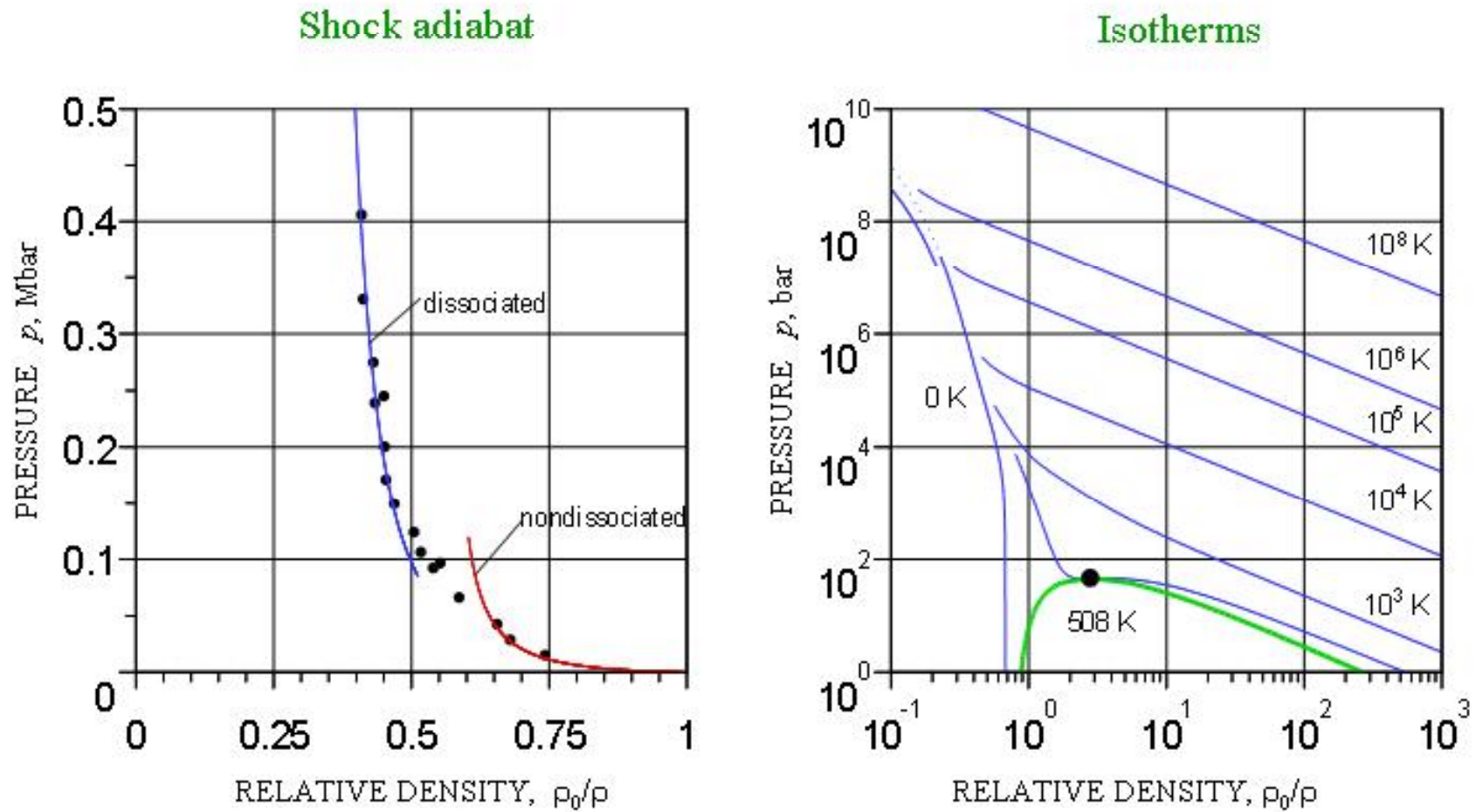
Figure 1

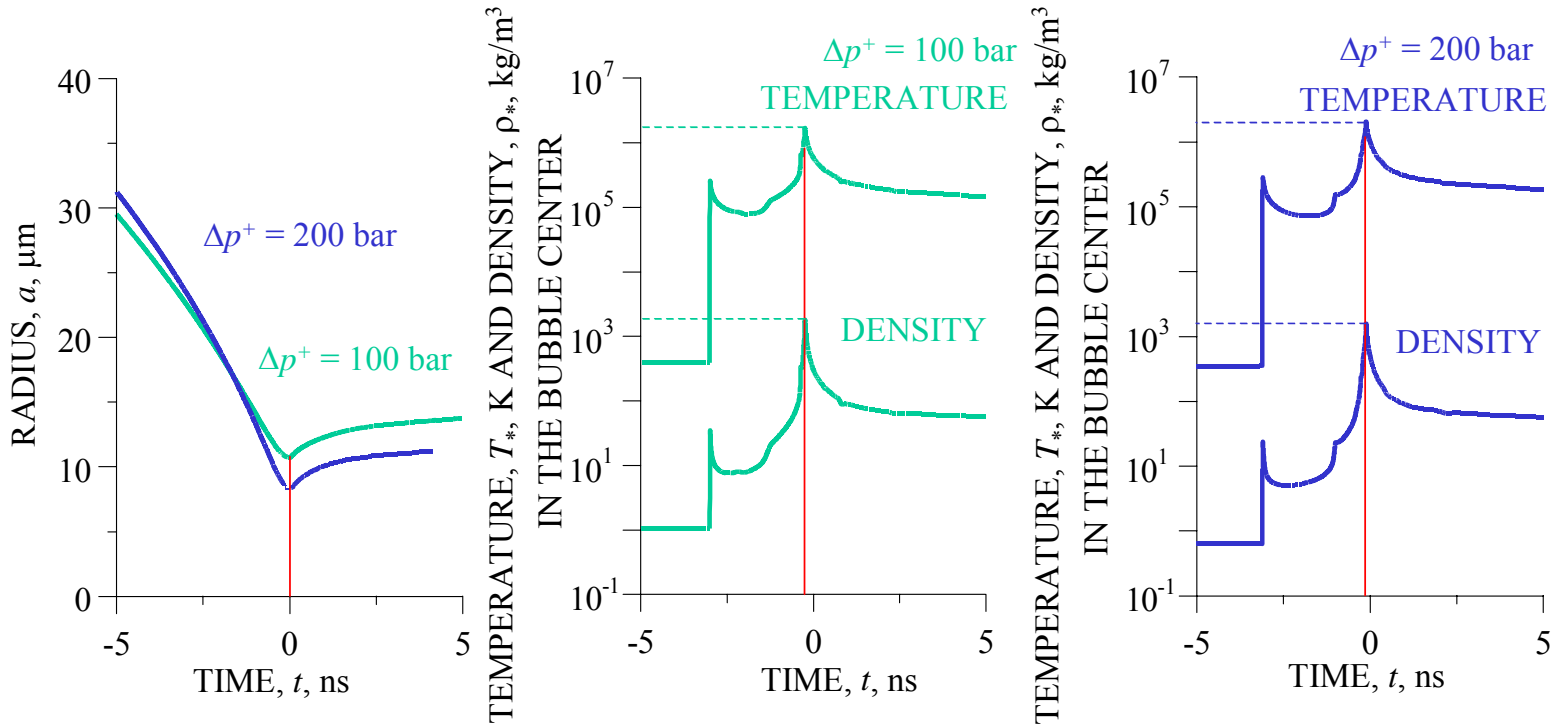## Vapor Bubble Collapse in Deuterated Acetone, C_3D_6O
(Low Mach Number Stage)

Bubble radius and vapor mass evolution at various amplitudes, Δp, of driving pressure.
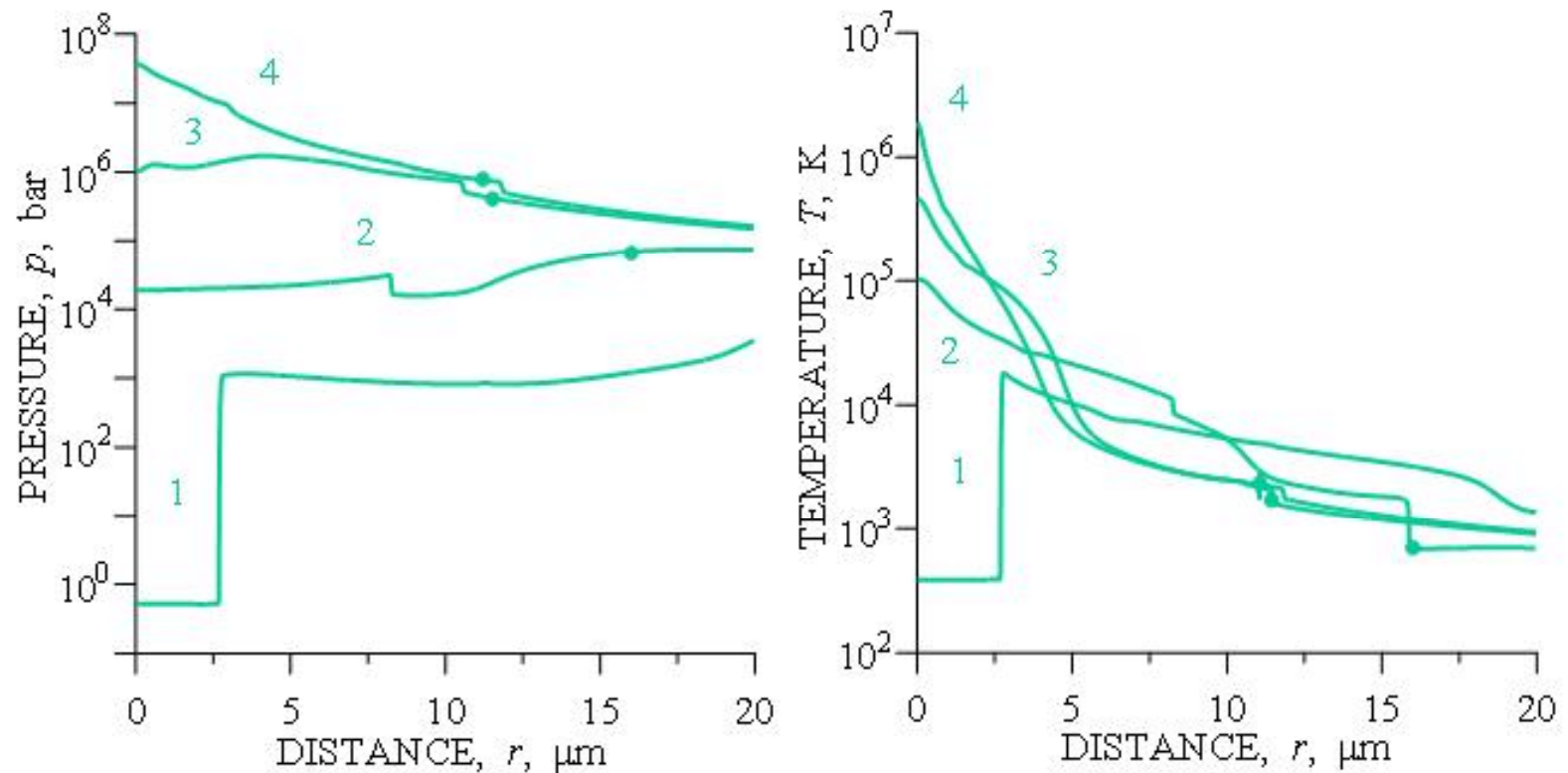$f = 20.5$ kHz, $T_0 = 273$ K, $\alpha = 1.0$.

Figure 2

13

Vapor Bubble Collapse in Deuterated Acetone, C_3D_6O
(High Mach Number Stage)

Temperature and density evolution of acetone near the center of the bubble (at r= r*).
$f = 20$ kHz, $T_0 = 273$ K, $\alpha = 1.0$.

Figure 3

Vapor Bubble Collapse in Deuterated Acetone, C_3D_6O
(High Mach Number Stage)

Pressure and temperature spatial distributions in the bubble.

$\Delta p^+ = 100$ bar, $f = 20.5$ kHz, $T_0 = 273$ K, $\alpha = 1.0$.

Figure 4